

---

Oral presentation | Numerical methods

## Numerical methods-V

Wed. Jul 17, 2024 4:30 PM - 6:30 PM Room A

---

### [9-A-03] Implementation and Analysis of a KEEP Scheme for Numerical Simulations of the Navier-Stokes Equations

Andrew Heletkanycz<sup>1</sup>, \*James George Coder<sup>1</sup> (1. The Pennsylvania State University)

Keywords: Kinetic energy preservation, Entropy preservation, Entropy stability

# Implementation and Analysis of a KEEP Scheme for Numerical Simulations of the Navier-Stokes Equations

Andrew Heletkanycz and James Coder  
Corresponding author: avh5950@psu.edu  
The Pennsylvania State University, USA.

**Abstract:** Kinetic energy and entropy preserving (KEEP) schemes are attractive for discrete satisfaction of entropy and kinetic energy conservation. This ensures their inherent stability without the need for solution stabilization strategies like artificial dissipation or filtering. A new KEEP-like scheme is proposed using entropy-variable analysis. An isentropic convecting vortex and the viscous Taylor-Green vortex were used to evaluate the performance of the proposed scheme. Two existing kinetic-energy and approximate entropy preserving were used as a comparison. Both test cases show that the proposed scheme performs similarly to the existing KEEP schemes and exhibits the expected stability. To display the effect of artificial solution stabilization, the proposed KEEP scheme was used with filtering to simulate a viscous Taylor-Green vortex. Including filtering led to a substantial reduction of enstrophy in the solution.

*Keywords:* Kinetic energy preservation, Entropy preservation, Entropy stability

## 1 Introduction

The desire for higher order, stable, and physically consistent flow simulations has been a driving force behind the development of schemes for fluid simulations, but there has always been a trade off between stability and accuracy. A classic example is modeling shock waves. Where there is a shock waves present, there are large gradients present, which lead to spurious oscillations when solved with the classic finite difference approximation. These oscillations are not realistic and can destabilize the solution, which, often times, causes the simulation to fail. To combat this, multiple methods have been proposed. One of the early ideas were monotonic schemes, the basic ideas of which were proposed by the work of Godunov [1]. Monotonic schemes are defined by two properties. They do not introduce new local extrema as the solution evolves and prevent already existing extrema, minima or maxima, from becoming more extreme. Monotonic schemes, such as the exact Riemann solver developed by Godunov [1] or approximate Riemann solvers (e.g., the Roe scheme [2]), can only be first order accurate, as stated by Godunov's theorem. As a result, discontinuities tend to be smeared over several grid points, which is not the infinitely thin shockwaves that the Navier Stokes equations predict.

Monotonic schemes are a subset of what are called total variation diminishing (TVD) schemes. These schemes preserve monotonicity, but can achieve higher orders of accuracy by using flux limiters. The MUSCL scheme, which stands for Monotonic Upstream-centered Scheme for Conservation Laws, was a TVD scheme proposed by Van Leer that is second order in for smooth solutions [3]. However, the scheme degrades to first order at large discontinuities, such as shocks. One type of scheme, proposed by Harten et al. [4] and Osher and Shu [5], that overcomes this shortcoming are essentially non-oscillatory (ENO) schemes, which are not in the family of TVD schemes. These schemes use multiple difference stencils and choose the stencil that has the least amount of oscillation while preventing the discontinuity from finding itself on a node. This yields schemes that minimize oscillations, are of higher order, and are of uniform order across the computational domain. An improvement to ENO schemes was proposed by Liu et al. named the weighted essentially non-oscillatory scheme (WENO) [6]. Instead of incorporating only one stencil in the solution, WENO schemes use a weighted combination of the stencils. This increases the order of accuracy of the scheme and decreases the spurious oscillations around shocks when compared to an ENO scheme with the same selection of stencils.

Another approach is suppress spurious oscillations and stabilize solutions is to add artificial dissipation by modifying the PDE to include additional even-order derivatives that scale with the grid spacing. The coefficients of the higher derivatives are usually specified by the user. These coefficients are case dependent, meaning that different situations and solver conditions require their own specific coefficient. Selecting too low of a value can lead to the simulation exhibiting oscillations or becoming too unstable

to run. On the other hand, choosing too high of a value contaminates the regions that are already dominated by viscous effects and can degrade inviscid features of the flow. A prominent example of artificial dissipation is the work of Jameson, Schmidt, and Turkel [7], who use an adaptive sensor to adjust the artificial dissipation coefficients so that high-order accuracy is maintained in smooth regions, but switches to first-order accuracy in the vicinity of shockwaves. Another method to remove spurious oscillations is to use a filter, such as the one suggested by Lundquist and Nordström [8]. This type of filter does not need to be tailored to every unique problem but still has the same shortfall of distorting features in the simulation.

Another method of achieving a stable scheme is to conserve kinetic energy, meaning that the scheme does not artificially add or remove kinetic energy from the simulation, like one proposed by Jameson. However, preserving kinetic energy alone is not enough to ensure stability for compressible flows [9]. Therefore, entropy also needs to be accounted for, making kinetic energy and entropy preserving (KEEP) schemes the next goal. KEEP schemes, such as those proposed by Chandrashekar [10] and Kuya et al. [11], discreetly conserve kinetic energy and satisfy the entropy condition, e.i. the second law of thermodynamics. As a result, these schemes are inherently stable without the need of artificial dissipation or filtering and satisfy the laws of physics from point to point.

This paper proposes a new KEEP-like scheme using entropy-variable analysis following Chandrashekar's approximate entropy flux [10]. This scheme, along with schemes by Chandrashekar and Kuya et al., were used to simulate a two-dimensional, periodic-convecting, isentropic vortex governed by the Euler equations to determine the behavior of the scheme on a curvilinear mesh. A viscous Taylor-Green vortex simulation on grid resolutions of  $193^3$  and  $256^3$  was also conducted to analyze the proposed scheme's properties with respect to a direct numerical simulation solution.

## 2 Kinetic Energy and Entropy Preservation

The compressible Navier-Stokes equations express the conservation of mass, momentum, and energy for a fluid control volume. They may be written hyperbolic conservation law of the form,

$$\frac{\partial q}{\partial t} + \frac{\partial f_j}{\partial x_j} = 0 \quad (1)$$

where  $q$  is the vector of conserved variables  $[\rho, \rho u_i, \rho e_0]$ , and  $f_j$  contains the fluxes acting on the surface surrounding the control volume. In this work, focus is restricted to an ideal, calorically perfect gas for which

$$P = \rho RT \quad (2)$$

and

$$T = (\gamma - 1) \left[ e_0 - \frac{1}{2} (u^2 + v^2 + w^2) \right] \quad (3)$$

Directly discretizing the form of Eq. 1 allows the underlying conservation laws to be satisfied in a discrete sense. This is done by constructing

$$\frac{\partial f}{\partial x} \approx \frac{f_{i+1/2}^* - f_{i-1/2}^*}{\Delta x} \quad (4)$$

This form is consistent with the very notion of conservation where fluxes on a control surface are shared by the control volumes adjoining that surface. However, this form does not guarantee that auxiliary functionals that follow from the continuous form of the equations are themselves discretely satisfied. This is because that any reasonable convex combination of the state variables can be used to define the interfacial flux  $f_{i+1/2}^*$ . Rather, additional constraints are required when defining  $f_{i+1/2}^*$  to ensure that it discretely mimics the desired behavior.

Broadly speaking, the advection of an auxiliary functional  $\mathcal{U}$  can be defined constructed as

$$\frac{\partial \mathcal{U}}{\partial t} + \frac{\partial \mathcal{F}_j}{\partial x_j} = \mathcal{V}^T \left( \frac{\partial q}{\partial t} + \frac{\partial f_j}{\partial x_j} \right) \quad (5)$$

where

$$\mathcal{V} = \frac{\partial \mathcal{U}}{\partial q} \quad (6)$$

and  $\mathcal{F}_j$  is the total flux of the  $\mathcal{U}$ . Integrating the spatial term of Eq. 5 from one-point to another in the

domain, such as across a control volume interface yields,

$$\Delta(\mathcal{F}) = \Delta(\mathcal{V}^T f) - \Delta(\mathcal{V})^T f^* \quad (7)$$

where  $f^*$  is a suitably defined average flux along the path of integration, i.e.

$$f^* = \begin{bmatrix} f^{*,\rho} \\ f^{*,m} + \tilde{P} \\ f^{*,e} \end{bmatrix} \quad (8)$$

## 2.1 Kinetic Energy Preservation

An auxiliary function of great interest for discrete conservation is the kinetic energy of the flow. This is especially the case for turbulent, where the kinetic energy contained at different length scales and the transfer of energy between length scales mediates the flow. Thus setting

$$\mathcal{U} = \rho K = \frac{1}{2} \rho (u^2 + v^2 + w^2) \quad (9)$$

leads to  $\mathcal{V}^T = [-K, u, v, w, 0]$ . Per Jameson [12], the advection of kinetic energy is discretely satisfied if,

$$f_{i+1/2}^{*,m} = \bar{u}_{i+1/2} f_{i+1/2}^{*,\rho} \quad (10)$$

where  $\bar{u}_{i+1/2}$  is the arithmetic average of  $u_i$  and  $u_{i+1}$ . Although Jameson suggests definitions of  $f^\rho$ ,  $\tilde{P}$ , and  $f^e$  [12], Chandrashekar [10] points out that there are no restrictions on these quantities. Rather, the condition in Eq. 10 is necessary and sufficient.

## 2.2 Entropy Conservation and Consistency

A further constraint on the discrete flux is to require that it discretely satisfy the transport of thermodynamic entropy through the domain. By convention, it is defined that  $\mathcal{U} = -\rho s$ , where  $s$  is the specific thermodynamic entropy. The resulting entropy variables are

$$\mathcal{V}^T = \left[ C_p - s - \frac{V^2}{2T}, \frac{u}{T}, \frac{v}{T}, \frac{w}{T}, -\frac{1}{T} \right] \quad (11)$$

If one considers integration normal to the control surface, the resulting condition for entropy conservation is

$$\Delta(\rho u) = \Delta(\mathcal{V})^T f^* \quad (12)$$

However, it should be noted that satisfying this condition does not necessarily make a flux entropy *consistent*, as it does not account for the entropy production through a shockwave.

### 2.2.1 Ismail-Roe Flux

Ismail and Roe [13] approach the question of entropy conservation by taking a path similar to the classical Roe flux. Using 1D flow, they define three additional variables,

$$z_1 = \sqrt{\frac{1}{T}}, \quad z_2 = u \sqrt{\frac{1}{T}}, \quad z_3 = \rho \sqrt{T} \quad (13)$$

that allow the conservative variables and the fluxes to all be quadratic, e.g.,

$$C_p - s - \frac{u^2}{2T} = C_p + C_v \ln z_1^2 + R \ln z_1 z_3 - \frac{z_2^2}{2}, \quad \frac{u}{T} = z_1 z_2, \quad -\frac{1}{T} = -z_1^2 \quad (14)$$

The entropy conservation equation may then be expanded into terms that are all linear in either  $\Delta z_1$ ,  $\Delta z_2$ , or  $\Delta z_3$ . After equating all terms with the same jump, they obtained

$$f^{*,\rho} = \bar{z}_2 \hat{z}_3 \quad (15)$$

where the overhat denotes a logarithmic average, and

$$f^{*,m} = \frac{\overline{z_2^2} \hat{z}_3}{z_1} \neq \bar{u} f^{*,\rho} \quad (16)$$

It is important to note that the Ismail-Roe momentum flux is not consistent with the Kinetic Energy Preserving condition developed by Jameson.

### 2.2.2 Chandrashekar Exact Kinetic Energy and Entropy Conserving Flux

In a subsequent development by Chandrashekar [10], a numerical flux that is both kinetic energy preserving and exactly entropy conserving was derived. In the construction of this flux, the Jameson constraint was imposed at the outset of the derivation. Rather than following the approach of Ismail and Roe, Chandrashekar focused on the jumps  $\Delta\rho$ ,  $\Delta u$ , and  $\Delta\frac{1}{T} = \Delta\beta$ . By equating terms linear in the respective jumps, Chandrashekar derives,

$$f^{*,\rho} = \hat{\rho}\bar{u} \quad (17)$$

$$f^{*,m} = \hat{\rho}\bar{u} \quad (18)$$

$$\tilde{P} = \frac{\bar{\rho}R}{\beta} \quad (19)$$

$$f^{*,e} = \left[ \frac{C_v}{\hat{\beta}} - \frac{\overline{u^2}}{2} \right] f^{*,\rho} + \bar{u} f^{*,m} + \bar{u}\tilde{P} \quad (20)$$

Again, the overhat is used to denote a logarithmic average, which takes the form,

$$\hat{\phi} = \frac{\Delta\phi}{\Delta\ln\phi} \quad (21)$$

### 2.2.3 Chandrashekar Exact Kinetic Energy and Approximate Entropy Flux

Also in Ref. [10], Chandrashekar presents a flux that exactly preserves kinetic energy and approximately conserves entropy. The construction is simple, and can be obtained by replacing the logarithmic averages with arithmetic averages. The resulting error in entropy conservation is  $\mathcal{O}(\Delta\rho^3) + \mathcal{O}(\Delta\beta^3)$ .

### 2.2.4 Kinetic Energy and Entropy Preserving (KEEP) Schemes

Another class of schemes in this realm are the so-called Kinetic Energy and Entropy Preserving (KEEP) schemes, originally proposed by Kuya et al. [11] and Kuya and Kawai [14, 15]. The original formulation was inspired using the Gibbs relation to define an entropy equation. While this approach is fully consistent with using entropy variables in tandem with the kinetic-energy equation, the result does not offer an intuitive way to satisfy the constraints. Rather, Kuya et al. [11] define several analytical relations to constrain their construction. This ultimately leads the use of various quadratic and cubic split form approximations of the derivatives. However, it can be shown via entropy-variable analysis that the KEEP flux does not discretely conserve entropy. Rather, it contains errors that are cubic with respect to the jumps similar to Chandrashekar's approximate flux.

## 2.3 New KEEP-like Scheme

Through further investigation of the aforementioned schemes, it has been found that KEEP-type schemes can be constructed using entropy-variable analysis following Chandrashekar's approximate entropy flux [10]. Beginning with the statement of entropy conservation,

$$f^\rho \Delta v_1 + (f^\rho \bar{u} + \tilde{P}) \Delta v_2 + f^e \Delta v_3 = R(\bar{\rho} \Delta u + \bar{u} \Delta \rho) \quad (22)$$

the jump in entropy variables can be approximately represented as

$$\Delta v_1 = -\Delta s - \Delta\left(\frac{u^2}{2T}\right) = -\frac{C_v}{T} \Delta T + \frac{R}{\bar{\rho}} \Delta \rho - \frac{\bar{u} \Delta u}{T} + \frac{\overline{u^2}}{2\bar{T}^2} \Delta T + \mathcal{O}(\Delta\rho^3) + \mathcal{O}(\Delta T^3) + \mathcal{O}(\Delta u \Delta T^2)$$

$$\begin{aligned}\Delta v_2 &= \frac{\Delta u}{T} - \frac{\bar{u}}{T^2} \Delta T + \mathcal{O}(\Delta T^3) + \mathcal{O}(\Delta u \Delta T^2) \\ \Delta v_3 &= \frac{1}{T^2} \Delta T + \mathcal{O}(\Delta T^3)\end{aligned}$$

This variation of the scheme uses  $-\frac{\Delta T}{T^2}$  as opposed to  $\Delta(\frac{1}{T})$  used by Chandrashekar.

By collecting like terms of  $\Delta\rho$ ,  $\Delta u$ , and  $\Delta T$ , expressions for  $f^\rho$ ,  $\tilde{P}$ , and  $f^e$  are may be obtained in a straightforward manner as,

$$f^\rho = \bar{u}\bar{\rho} \quad (23)$$

$$\tilde{P} = R\bar{\rho}\bar{T} \quad (24)$$

$$f^e = f^\rho(\bar{u}^2 - \frac{1}{2}u^2 + C_v\bar{T}) + \bar{u}\tilde{P} \quad (25)$$

respectively. While the natural solution to the relations involves the arithmetic mean of the density, recent work by de Michele and Coppola suggests that using the geometric mean of the density,  $\tilde{\rho} = \sqrt{\rho_i\rho_{i+1}}$  can reduce the errors in entropy [16]. This result is used here, hence the numerical inviscid flux of the new scheme takes the form,

$$f_{i+1/2}^* = \begin{bmatrix} \tilde{\rho}\bar{u} \\ \tilde{\rho}\bar{u}^2 + \tilde{\rho}R\bar{T} \\ \tilde{\rho}\bar{u}\left(\bar{u}^2 - \frac{1}{2}u^2 + C_p\bar{T}\right) \end{bmatrix} \quad (26)$$

## 2.4 Curvilinear Coordinates

Considering now the kinetic energy and entropy conditions for the governing equations written in generalized curvilinear coordinates, i.e.,

$$\frac{\partial J^{-1}q}{\partial t} + \frac{\partial \hat{F}}{\partial \xi} + \frac{\partial \hat{G}}{\partial \eta} = 0 \quad (27)$$

in two spatial dimensions, with

$$\hat{F} = \begin{bmatrix} \rho U \\ \rho u U + J^{-1}\xi_x P \\ \rho v U + J^{-1}\xi_y P \\ \rho h_0 U \end{bmatrix} \quad (28)$$

in which  $U = J^{-1}(\xi_x u + \xi_y v)$  is the contravariant velocity. As with the Cartesian case, the auxiliary relations can be satisfied by multiplying by the auxiliary variable set (e.g., the entropy variables) and integrating by parts between nodes or across a cell interface, leading to

$$\begin{aligned}R\Delta(\rho U) &= \Delta\left(C_p - s - \frac{u^2 + v^2}{2T}\right)(\rho U) + \Delta\left(\frac{u}{T}\right)(\rho u U + J^{-1}\xi_x P) \\ &+ \Delta\left(\frac{v}{T}\right)(\rho v U + J^{-1}\xi_y P) - \Delta\left(\frac{1}{T}\right)(\rho h_0 U)\end{aligned} \quad (29)$$

The same cancellation strategy can be employed as with the Cartesian case, leading to

$$\hat{F}_{j+1/2}^* = \begin{bmatrix} \tilde{\rho}\bar{U} \\ \tilde{\rho}\bar{u}\bar{U} + \frac{\tilde{\rho}\bar{U}}{J^{-1}\xi_x}\tilde{P} \\ \tilde{\rho}\bar{v}\bar{U} + \frac{\tilde{\rho}\bar{U}}{J^{-1}\xi_y}\tilde{P} \\ \tilde{\rho}\bar{U}\left(\bar{u}^2 + \bar{v}^2 - \frac{1}{2}u^2 + v^2 + C_p\bar{T}\right) \end{bmatrix} \quad (30)$$

However, there remains slight ambiguity in the definition of the averaged contravariant velocity  $\bar{U}$ . Integrating between nodes suggests that this should be defined as the arithmetic average of the contravariant velocities, but this leads to entropy errors that are linear with respect to the change in grid metrics. Instead, it is defined that

$$\bar{U} = \overline{J^{-1}\xi_x u} + \overline{J^{-1}\xi_y v} \quad (31)$$

where the overlines represent arithmetic averages. This definition is more consistent with a finite-volume approach than a finite-difference approach. While this may seem subtle, it affects the eventual construction of higher-order KEEP-like schemes.

### 3 Implementation

The new KEEP scheme was implemented in an in-house Wall-Resolved Body-fitted Large-Eddy Simulation (WRBLES) code. WRBLES is a single-block, structured-grid solver that currently incorporates a bandwidth-optimized 7-point, 4th-order central difference scheme that satisfies the summation-by-parts convention [17]. Viscous fluxes are constructed at each point by applying the same SBP finite-difference operator to the primitive variables, and subsequently combined with the inviscid flux before differencing. Boundary conditions are enforced using Roe fluxes [2] with an entropy fix applied to the inviscid eigenvalues and an estimate of the viscous spectral radius added in. Periodic boundaries are treated using the finite-domain formulation with a common interface flux at the endpoints. The baseline version of the solver uses conventional central differencing, and thus requires additional stabilization. The code is capable of both artificial dissipation and filtering, and typical operation employs an 8th-order Lundquist-Nordstrom-type filter [8] with 4th-order boundary contributions that is symmetric positive definite with respect to the mass matrix of the baseline differencing scheme.

The new KEEP scheme described above was implemented for in a second-order-accurate manner for all interior interfacial fluxes. The boundary-condition enforcement and treatment of viscous fluxes was unaltered. Although filtering remains available, it is optional as the KEEP scheme does not require filtering to remain stable.

Time advancement in WRBLES is implicit using a 2nd-order accurate ESDIRK scheme [18] with inversions performed using the LU-SGS scheme of Yoon and Jameson [19]. Newton-type subiterations are used to reduce solution error. In practice, 3-5 subiterations are used per stage to handle high-resolution cells and ensure sufficient update of the boundaries. No modifications were found to be necessary for use with the KEEP scheme.

## 4 Numerical Results

### 4.1 Convecting Isentropic Vortex

A second, more complicated, test case considered was that of a two-dimensional, periodic-convecting, isentropic vortex governed by the Euler equations,

$$\frac{\partial \rho}{\partial t} + \frac{\partial \rho u_j}{\partial x_j} = 0 \quad (32)$$

$$\frac{\partial \rho u_i}{\partial t} + \frac{\partial \rho u_i u_j + P \delta_{ij}}{\partial x_j} = 0 \quad (33)$$

$$\frac{\partial \rho e_0}{\partial t} + \frac{\partial \rho u_j h_0}{\partial x_j} = 0 \quad (34)$$

for an ideal, calorically perfect gas with  $\gamma = 1.4$ . The specific initial conditions used in this test case were,

$$u = M_\infty - \frac{V_s}{2\pi} y e^{G_s(1-r^2)} \quad (35)$$

$$v = \frac{V_s}{2\pi} x e^{G_s(1-r^2)} \quad (36)$$

$$T = \frac{1}{\gamma} - \frac{V_s^2(\gamma-1)}{16G_s\gamma\pi^2} e^{2G_s(1-r^2)} \quad (37)$$

$$\rho = (\gamma T)^{\frac{1}{\gamma-1}} \quad (38)$$

where  $r^2 = x^2 + y^2$ . Following the work of Pulliam[20], it was specified that  $M_\infty = 0.5$ ,  $G_s = 0.5$ , and  $V_s = 5$ .

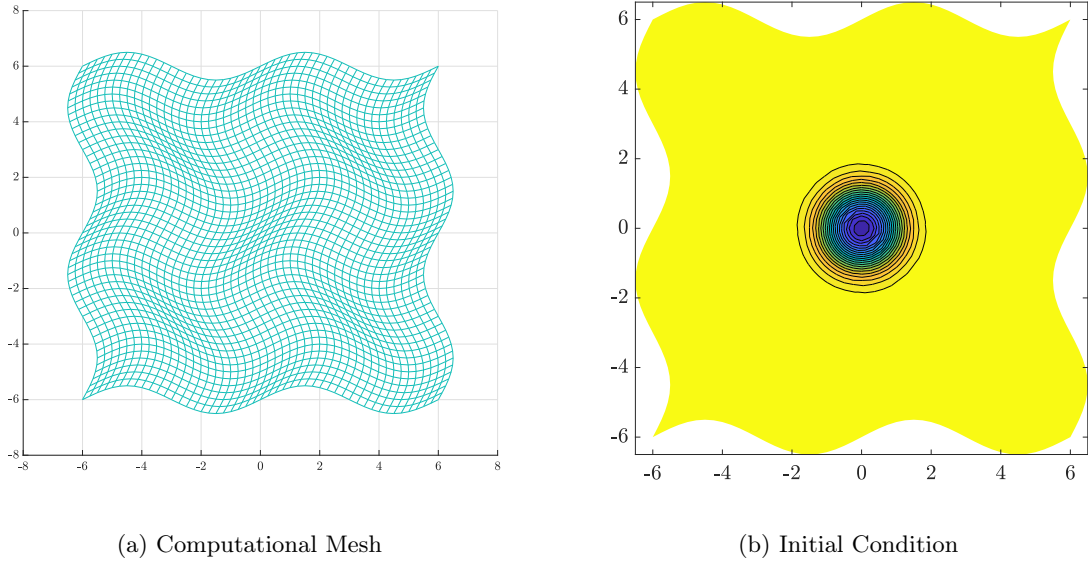


Figure 1: Mesh and initial condition periodic convecting vortex case.

The system was simulated on a curvilinear mesh defined by,

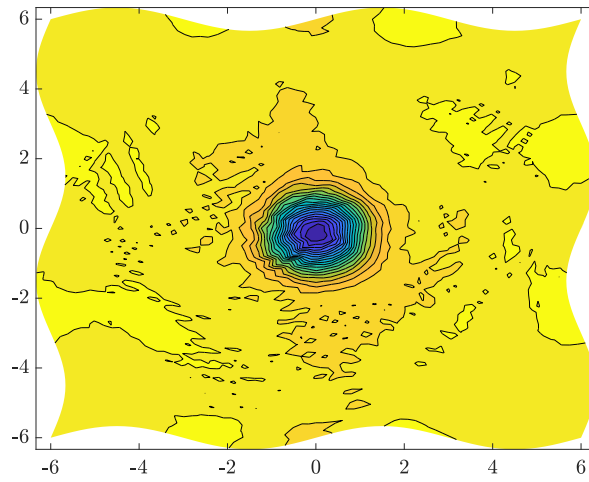
$$x = -6 + \frac{12}{j_{max}} \left[ j + A_x \sin(2\pi\kappa) \sin\left(\frac{\lambda\pi k}{k_{max}}\right) \right] \quad (39)$$

$$y = -6 + \frac{12}{k_{max}} \left[ k + A_y \sin(2\pi\kappa) \sin\left(\frac{\lambda\pi j}{j_{max}}\right) \right] \quad (40)$$

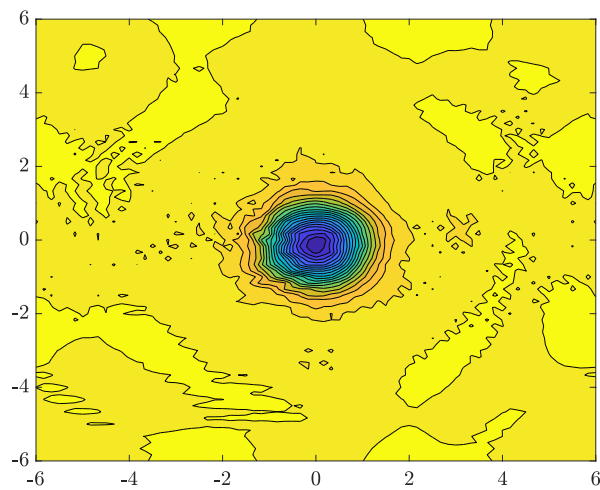
with  $A_x = A_y = 2$ ,  $\lambda = 4$ ,  $\kappa = 0.25$ , and  $j_{max} = k_{max} = 72$  (corresponding to an average spacing in both directions of  $\Delta s_{avg} = 1/6$ ). The resulting mesh is pictured below in Fig. 1 along with contours of density for the initial conditions. The governing equations were recast into generalized curvilinear coordinates following Pulliam and Steger [21] with analytic grid metrics and discretized using the curvilinear version of the new KEEP scheme with truly periodic boundaries. As the analytic grid metrics do not discretely satisfy a geometric conservation law, the numerical fluxes based on free-stream quantities are subtracted from the residual. The equations were advanced using a 3rd-order explicit Runge-Kutta scheme with  $\Delta t = 1/30$  (an average CFL of approximately 0.2).

The predicted density contours after one convective period (720 time steps) are shown in Fig. 2. Also included are results from a Cartesian mesh of the same baseline size to confirm that the approximate treatment of grid metrics does not contaminate the solution. It is important to remember that these solutions are for a 2nd-order accurate central scheme without any dissipation (viscous or artificial) or filtering. Thus, oscillations in the contours are to be expected.

The time histories of the integrated kinetic energy and thermodynamic entropy for the convective period are shown in Fig. 3 for the new KEEP flux along with the exactly entropy preserving Chandrashekar flux [10] the original KEEP scheme of Kuya et al. [11]. Also included is the entropy history from Cartesian mesh solutions using the same flux definitions to isolate the influence of grid metrics. The integrated kinetic energy of all three schemes oscillates, but this is to be expected since this is a compressible flow case and the KEP condition focuses only on advection and not the pressure work term. The thermodynamic entropy of all schemes oscillates at very similar levels. This is regarded as being due to the analytic grid metrics not being discretely conservative, as the Kuya KEEP scheme handles grid metric variations differently than the new KEEP scheme, and that the Cartesian-grid results have much less variation over the time history. In the Cartesian results, the Chandrashekar flux results show a monotonic increase in thermodynamic entropy, which is an effect of the 3rd-order Runge-Kutta scheme being slightly dissipative. The new KEEP scheme shows greater entropy than the original KEEP scheme; however, the original KEEP scheme shows a much stronger violation of the entropy condition around  $t = 14$ .

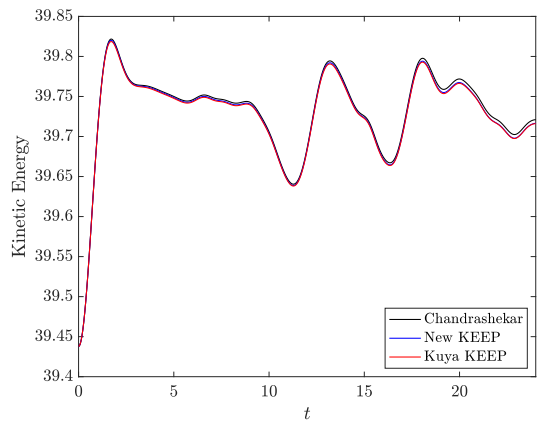


(a) Curvilinear Mesh

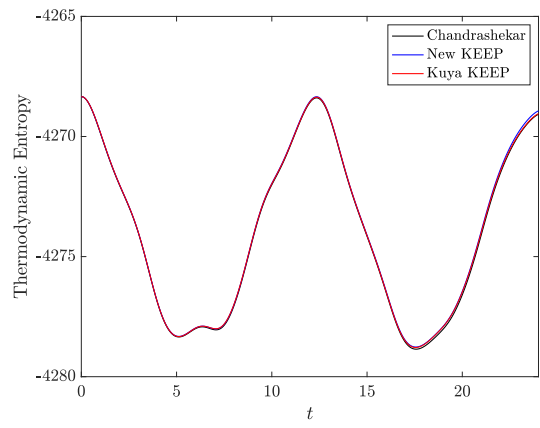


(b) Cartesian Mesh

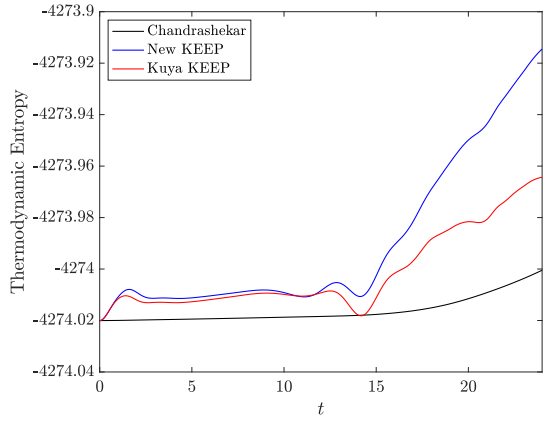
Figure 2: Mesh and initial condition periodic convecting vortex case.



(a) Kinetic Energy



(b) Entropy



(c) Entropy (Cartesian Reference)

Figure 3: Density contours after one convective period using the new KEEP scheme.

## 4.2 Taylor-Green Vortex

The viscous Taylor-Green vortex test was used a test case and was run on a  $193^3$  and  $256^3$  point grid at a mach number of 0.1 and a Reynolds number of 1,600 based on the domain width of  $2\pi$ . The initial conditions for the test case are outlined by Wang et al. [22]. The unfiltered KEEP scheme was compared to the finite difference scheme with filtering, results from a direct numerical simulation using a spectral element solver reported by Wang et al. [22], and solutions calculated with existing KEEP schemes.

### 4.2.1 Unfiltered KEEP Scheme Results

The simulations were run from initialization to a non-dimensionalized time of  $\frac{t}{t_c} = 20$ , where  $t_c$  is  $\frac{L}{V_0}$ . Figure 4 shows the evolution of kinetic energy and enstrophy as calculated by,

$$E = \frac{1}{\rho_0 \Omega} \int_{\Omega} \rho \frac{\mathbf{u} \cdot \mathbf{u}}{2} d\Omega \quad (41)$$

$$\mathcal{E} = \frac{1}{\rho_0 \Omega} \int_{\Omega} \rho \frac{\boldsymbol{\omega} \cdot \boldsymbol{\omega}}{2} d\Omega \quad (42)$$

where  $\mathbf{u}$  and  $\boldsymbol{\omega}$  are velocity and vorticity vectors, respectively. In the enstrophy plot, all simulations follow the same general trend that the reference spectral element simulation outlines with significant deviations higher or lower than the true value. All simulations agree well with the spectral element solution up until  $t \approx 3.6$ . The KEEP scheme solutions tend to overshoot the reference solution while the finite difference solutions tend to undershoot the reference solution. In both cases, as grid resolution increases, the solutions begin to approach the reference solution.

In the kinetic energy plot, all solutions closely follow the same trend as the reference spectral element solution with a minimal amount of deviation. Figure 4 shows the deviation of the simulations from the spectral element solution. Unlike the enstrophy plot, there are no general trends to notice except that the simulations again remain close until  $t \approx 3.6$ . Overall, the evolution of the kinetic energy predicted by the proposed keep scheme agrees very well with spectral element solution with the 256-grid-point solution slightly overestimating the true value.

In Figure 5, vorticity visualizations of the upper right quadrant of the mid y plane for different simulations at  $t = 8$  are shown.  $t = 8$  was chosen because this is about where maximum dissipation occurs and the smallest vorticities are present. The simulations each have of a ring of vorticity found near the upper left and lower right corners of each image, with coherence and shape varying with grid resolution and scheme used. In the KEEP simulations, odd-even decoupling is present. However, with a higher grid resolution, the amount of decoupling decreases significantly. It is also important mention that the KEEP scheme was used without filtering or dissipation and, even with odd-even decoupling, the simulation remained stable. The rings of vorticity are also more clearly defined at the higher grid resolution. In the simulations using the finite difference scheme, there is no odd-even decoupling, which is due to the use of a filter. It can also be argued that, when compared to the KEEP scheme simulations, the finite difference scheme has structures and gradients that are less sharp. This is best observed by the line of vorticity that runs diagonally and connects the two rings. This line is more clearly defined and thinner in the KEEP scheme simulation than in the finite difference simulation.

Overall, the second order unfiltered KEEP scheme performs very well. Although, the scheme does over predict the evolution and retention of enstrophy once the flow breaks down into turbulence. However, the enstrophy approaches the spectral element solution when the resolution of the grid is increased. The amount of odd-even decoupling also decreases when a higher resolution grid is used. The kinetic energy also agrees very well with the reference solution. Unlike with the enstrophy, there is no general trend of over prediction or under prediction of the kinetic energy in the simulation for the KEEP or finite difference schemes. Both schemes over predict or under predict at different points of the simulation, which also changes between different grid resolutions.

### 4.2.2 Filtered KEEP Scheme Results

To gauge how filtering affects the simulations, the Taylor-Green vortex case was again simulated with the KEEP scheme, but with the 8th-order filter implemented in the WRBLES code. Figure 6 shows that using filtering greatly decreases the entropy present in the KEEP scheme simulations to about the same level as in the corresponding filtered finite difference solutions. Kinetic energy adheres more closely to the spectral element solution, as shown in Figure 6, but the deviation was small to start with.

Figure 7 shows that the odd-even decoupling has been removed but at the cost of losing the definition found in the unfiltered KEEP simulation. The sharper gradients seen in the unfiltered KEEP scheme cases are no longer present, with the diagonal line of vorticity found in center region of each image serving as a good gauge. When compared to Figure 5, the slice bares more similarity to the finite difference case than to the unfiltered KEEP scheme.

The use of a filter significantly diminishes the amount of enstrophy in the simulation. This showcases the benefit of using a KEEP scheme, as it does not need filtering or artificial dissipation to be stable. Kinetic energy prediction does improve slightly by including the filter, the 256 grid point case especially, but the deviation from the spectral element solution was already very minor.

### 4.2.3 Comparison Against Existing Schemes

Chandrashekar's [10] entropy conservative scheme and the original KEEP scheme Kuya et al. [11] were also used to simulate the Taylor-Green vortex and compared to the scheme proposed in this paper. Since all three schemes agree very closely with one another, the proposed scheme's solution is subtracted from the other schemes to aid in comparison, as shown in Figure 8. When analysing the enstrophy and kinetic energy on the higher resolution grid, it is clear that the schemes by Chandrashekar and Kuya et al. correlate more strongly than either of the existing schemes to the proposed one. On the lower resolution grids, these schemes do not exhibit the strong correlation amongst each other that is found on the higher resolution grids but stay bounded around the proposed scheme. This figure reinforces the fact that the proposed scheme is well in line with existing kinetic energy and entropy preserving schemes.

## 5 Conclusion and Future Work

A kinetic energy and entropy preserving scheme using entropy-variable analysis following Chandrashekar's approximate entropy flux was proposed [10]. The proposed scheme's properties were then demonstrated using a two-dimensional, periodic-convecting, isentropic vortex governed by the Euler equations and a viscous Taylor-Green vortex governed by the Navier-Stokes equations. The isentropic vortex test case showed similar performance to the original KEEP scheme by Kuya et al. [11]. Although, the new scheme predicted more entropy than the original scheme, the violation in the entropy condition at certain points was not as large. In the Taylor-Green vortex case, the proposed KEEP scheme was compared to a 4th order central difference non-KEEP scheme that was previously used in the in-house code, as well as a DNS spectral element solution. This demonstrated that the proposed KEEP-like scheme was stable but demonstrated higher enstrophy than the reference spectral element case regardless of the grid resolution. On the other hand, the existing finite difference scheme underestimated the enstrophy for all grid resolutions tested. Both these schemes modeled kinetic energy well with KEEP scheme on the 256-point grid overestimating kinetic energy the most. When filtering was added to the KEEP scheme, the enstrophy present was severely reduced to about the same levels as the finite difference results. This shows the benefit of using an inherently stable scheme. When compared against existing kinetic energy and entropy conserving schemes, the proposed scheme agrees very well and is almost indistinguishable when the enstrophy and kinetic energy are plotted.

Future work will focus on constructing higher order KEEP schemes and extending the current scheme to curvilinear coordinates. Unearthing or creating a test case that better differentiates the kinetic energy and entropy preserving schemes will help determine the properties of each scheme. Whether it is a new case that is less deterministic than the viscous Taylor-Green vortex, increasing or decreasing the grid resolution, or modifying simulation parameters is yet to be determined.

## References

- [1] Sergei K. Godunov and I. Bohachevsky. Finite difference method for numerical computation of discontinuous solutions of the equations of fluid dynamics. *Matematicheskij sbornik*, 47(89)(3):271–306, 1959.
- [2] P. L. Roe. Approximate riemann solvers, parameter, vectors and difference schemes. *Journal of Computational Physics*, Vol. 43, No. 2, 1981, pp. 357-372.
- [3] Bram van Leer. Towards the ultimate conservative difference scheme. v. a second-order sequel to godunov's method. *Journal of Computational Physics*, 32(1):101–136, 1979.

- [4] Ami Harten, Bjorn Engquist, Stanley Osher, and Sukumar R Chakravarthy. Uniformly high order accurate essentially non-oscillatory schemes, iii. *Journal of Computational Physics*, 71(2):231–303, 1987.
- [5] Chi-Wang Shu and Stanley Osher. Efficient implementation of essentially non-oscillatory shock-capturing schemes. *Journal of Computational Physics*, 77(2):439–471, 1988.
- [6] Xu-Dong Liu, Stanley Osher, and Tony Chan. Weighted essentially non-oscillatory schemes. *Journal of Computational Physics*, 115(1):200–212, 1994.
- [7] A. Jameson, Wolfgang Schmidt, and Eli Turkel. Numerical solution of the euler equations by finite volume methods using runge kutta time stepping schemes. In *14th Fluid and Plasma Dynamics Conference*, AIAA Palo Alto, CA, June 1981. AIAA Paper 2023-3862.
- [8] Tomas Lundquist and Jan Nordström. Stable and accurate filtering procedures. *Journal of Scientific Computing*, 82(16):15–35, 2020.
- [9] Albert E. Honein. *Numerical aspects of compressible turbulence simulations*. PhD thesis, Department of Mechanical Engineering of Stanford University, 2005.
- [10] Praveen Chandrashekar. Kinetic Energy Preserving and Entropy Stable Finite Volume Schemes for Compressible Euler and Navier-Stokes Equations. *Communications in Computational Physics*, 14(5):1252–1286, 2015.
- [11] Yuichi Kuya, Kosuke Totani, and Soshi Kawai. Kinetic energy and entropy preserving schemes for compressible flows by split convective forms. *Journal of Computational Physics*, 375:823–853, 2018.
- [12] Antony Jameson. Formulation of kinetic energy preserving conservative schemes for gas dynamics and direct numerical simulation of one-dimensional viscous compressible flow in a shock tube using entropy and kinetic energy preserving schemes. *Journal of Scientific Computing*, 34(2):188–208, Feb 2008.
- [13] Farzad Ismail and Philip L. Roe. Affordable, entropy-consistent euler flux functions ii: Entropy production at shocks. *Journal of Computational Physics*, 228(15):5410–5436, 2009.
- [14] Yuichi Kuya and Soshi Kawai. High-order accurate kinetic-energy and entropy preserving (keep) schemes on curvilinear grids. *Journal of Computational Physics*, 442:110482, 2021.
- [15] Yuichi Kuya and Soshi Kawai. A stable and non-dissipative kinetic energy and entropy preserving (keep) scheme for non-conforming block boundaries on cartesian grids. *Computers & Fluids*, 200:104427, 2020.
- [16] Carlo De Michele and Gennaro Coppola. Asymptotically entropy-conservative and kinetic-energy preserving numerical fluxes for compressible euler equations. *Journal of Computational Physics*, 492:112439, 2023.
- [17] J. G. Coder. Bandwidth-optimized summation-by-parts operators for high-resolution turbulent flow simulations. In *AIAA Aviation 2023 Forum*, San Diego, CA, June 2023. AIAA Paper 2023-3862.
- [18] Christopher A Kennedy and Mark H Carpenter. Diagonally Implicit Runge-Kutta Methods for Ordinary Differential Equations. A Review. Technical Report March, NASA TM-2016-219173, 2016.
- [19] Seokkwan Yoon and Antony Jameson. Lower-upper symmetric-gauss-seidel method for the euler and navier-stokes equations. *AIAA Journal*, 26(9):1025–1026, 1988.
- [20] Thomas H. Pulliam. High order accurate finite difference methods: as seen in overflow. *20th AIAA Computational Fluid Dynamics Conference*, AIAA Paper 2011–3851, Honolulu, HI, June 2011.
- [21] Thomas H. Pulliam and Joseph L. Steger. Implicit finite-difference simulations of three-dimensional compressible flow. *AIAA Journal*, 18(2):159–167, 1980.
- [22] Z.J. Wang, Krzysztof Fidkowski, Rémi Abgrall, Francesco Bassi, Doru Caraeni, Andrew Cary, Herman Deconinck, Ralf Hartmann, Koen Hillewaert, H.T. Huynh, Norbert Kroll, Georg May, Per-Olof Persson, Bram van Leer, and Miguel Visbal. High-order cfd methods: current status and perspective. *International Journal for Numerical Methods in Fluids*, 72(8):811–845, 2013.

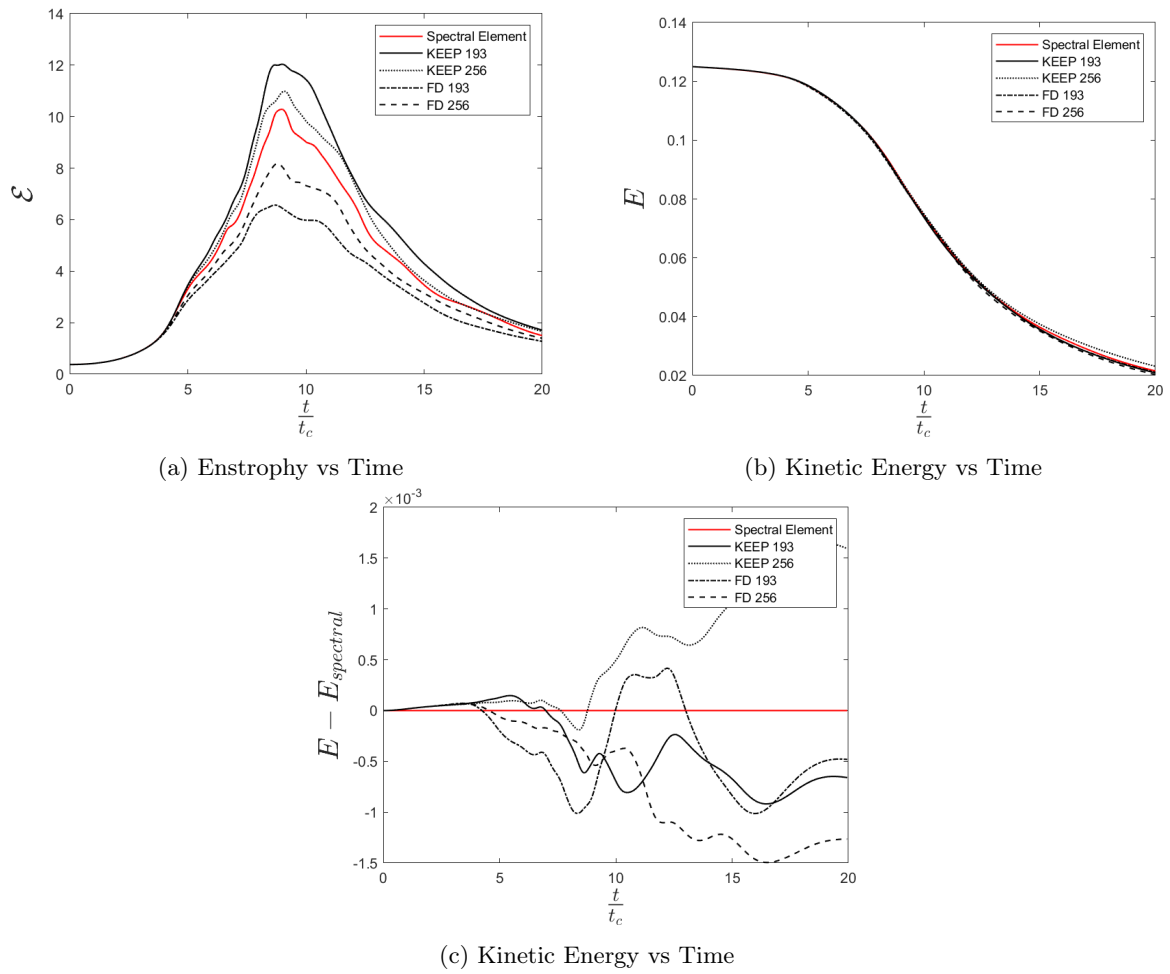


Figure 4: Plots of enstrophy and kinetic energy vs time of the unfiltered KEEP scheme, finite difference simulation, and the exact spectral element solution

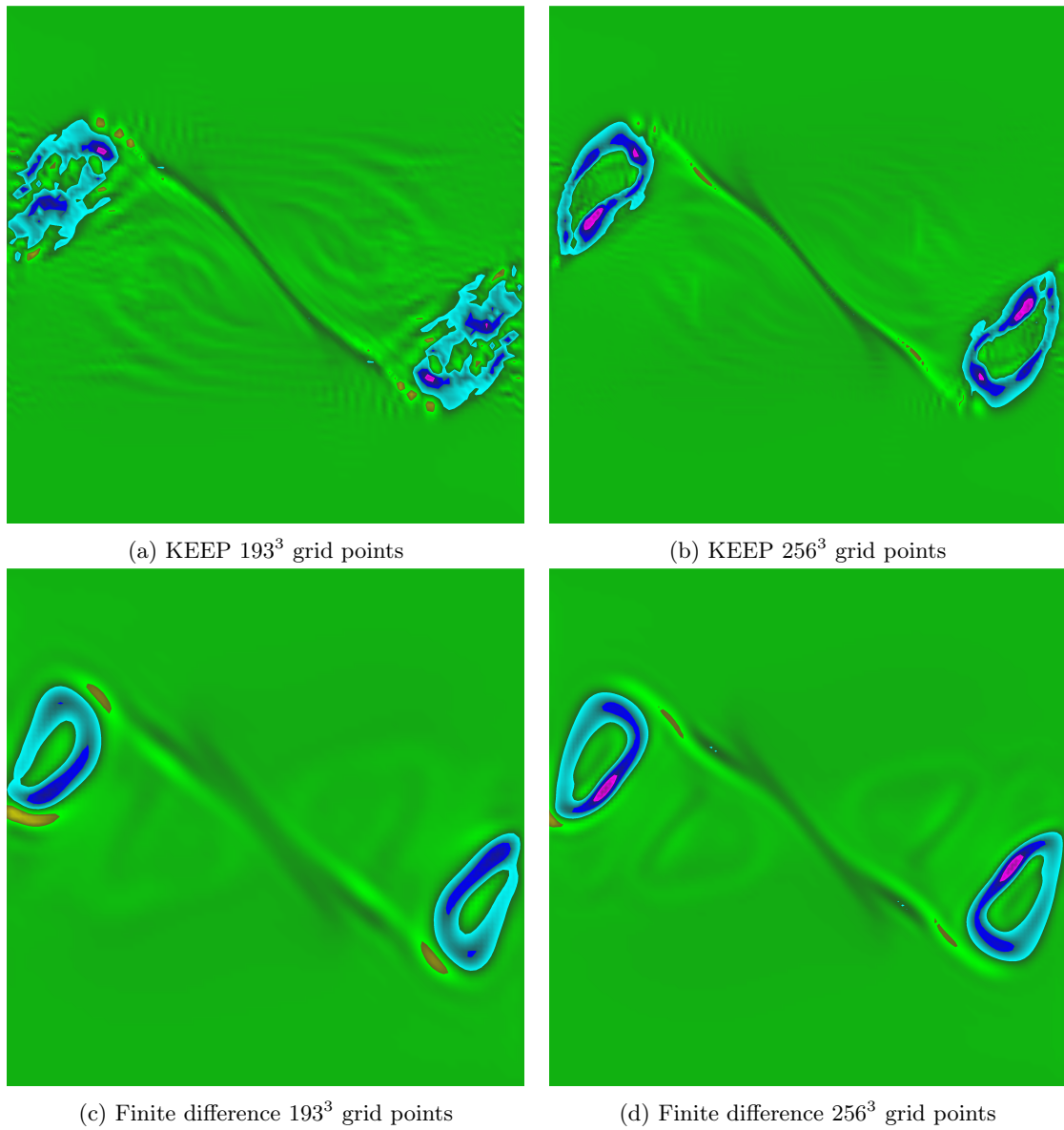


Figure 5: Vorticity visualizations of the upper right quadrant of the  $y = 0$  plane for different grid resolutions of the unfiltered KEEP and finite difference flux scheme

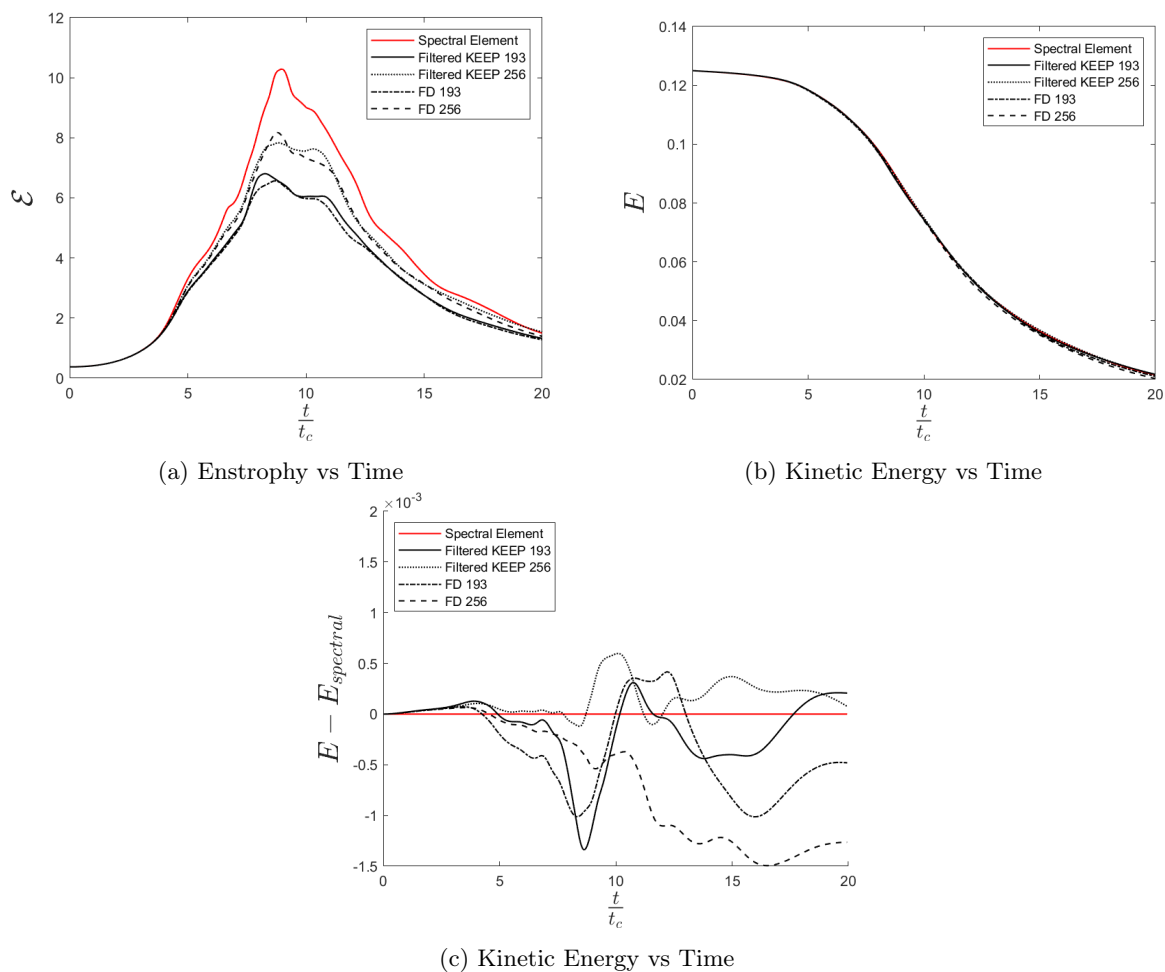


Figure 6: Plots of enstrophy and kinetic energy vs time of the filtered KEEP scheme, finite difference simulation, and the exact spectral element solution

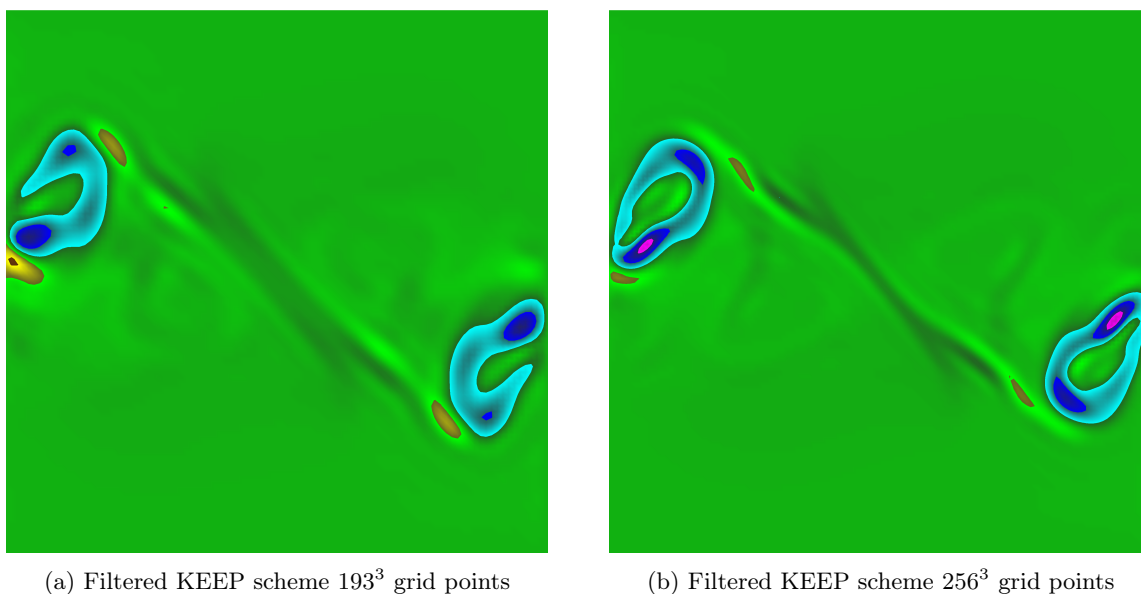
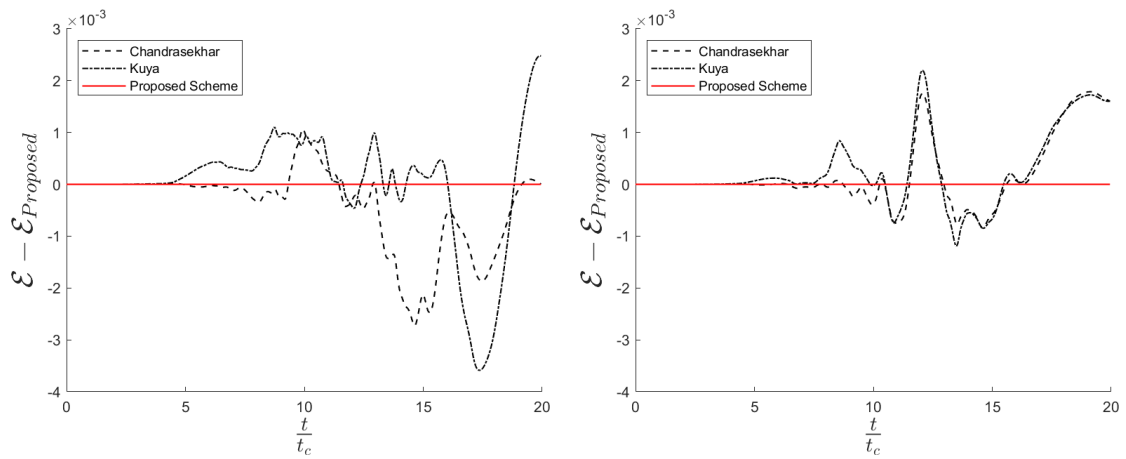
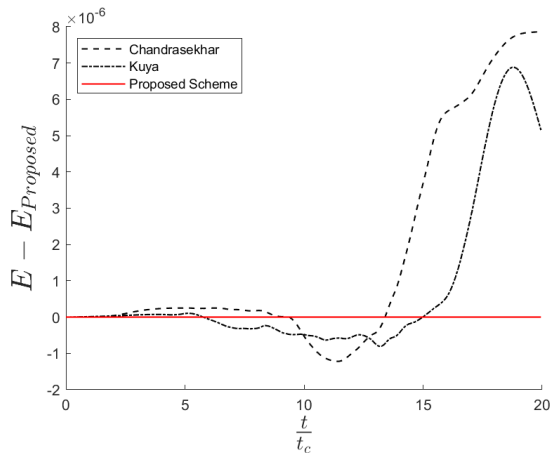


Figure 7: Vorticity visualizations of the upper right quadrant of the  $y = 0$  plane for different grid resolutions of the filtered KEEP and finite difference flux scheme

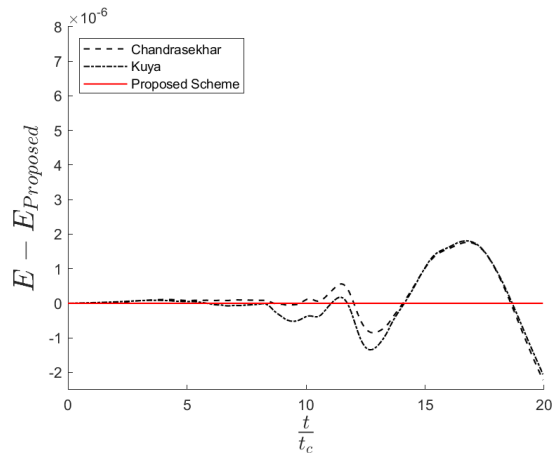


(a) Difference in enstrophy 193<sup>3</sup> grid points

(b) Difference in enstrophy 256<sup>3</sup> grid points



(c) Difference in kinetic energy 193<sup>3</sup> grid points



(d) Difference in kinetic energy 256<sup>3</sup> grid points

Figure 8: Plots of the difference of enstrophy and kinetic energy between the proposed scheme and schemes by Chandrasekhar and Kuya et al. simulated on different grid resolution